

3D-simulations of magnetic structures in af-coupled multilayers with pinholes

W. Schepper, K. Diplas, and G. Reiss

University of Bielefeld, Department of Physics, Universitätsstraße 25, 33501 Bielefeld, Germany

For antiferromagnetically (af) coupled Py (Ni₈₁Fe₁₉|Cu)-multilayers lattice calculations have been used already for the investigation of pinholes in GMR elements. The very thin spacer layer (<10 Å) is sensitive against pinholes as a link between the magnetic layers. Additional coupling through the pinhole modifies drastically the af-coupling between the magnetic layers and leads to strong changes in the $M(H)$ and $\Delta R/R(H)$ curves. Improved lattice calculations with large grids offer the opportunity, to study effects of geometry in layers structured laterally. © 2000 American Institute of Physics. [S0021-8979(00)86608-6]

I. INTRODUCTION

In the original work on pinholes¹ in magnetic multilayers showing af-coupling the magnetization was calculated in a rigid coupling model neglecting spin differences within a magnetic layer. Fulghum and Camley² introduced a lattice model including local field and Brillouin function. They obtained reliable results involving the linear af-coupling term. The influence of randomly distributed pinholes on the magnetization and GMR curves was analyzed by Kikuchi.³ In this work, we study the influence of pinholes on the magnetization and the GMR including both the bilinear as well as the biquadratic coupling and present an optimized geometry for the calculation.

II. LATTICE MODEL

Note, that we use natural units for Permalloy, i.e., with $J_N = 2.9 \times 10^{-14}$ erg the field is given by $H_N = B_N / \mu_0 = 1540$ kOe. Following the sketch of Fig. 1 and neglecting dipole interaction but including RKKY-af-coupling by the coupling constants (J_{al}, J_{aq}), the local field is given by

$$\vec{H}_{i,j,k} = \vec{H}_a + \sum_{i_l=1}^5 J_f \vec{S}_{i_l} + \vec{S}_6 \left\{ \begin{array}{ll} J_f & \text{f} \\ J_{al} + 2J_{aq} |S_{i,j,k}| |S_6| \cos(\alpha_{i,j,k} - \alpha_6) & \text{af} \end{array} \right. \quad (1)$$

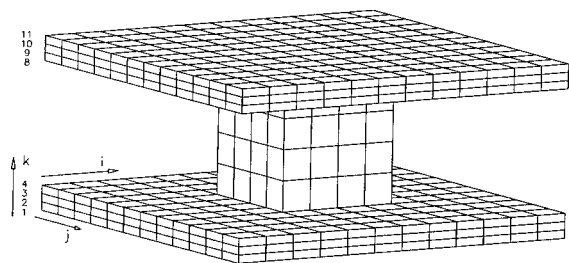


FIG. 1. Sketch of two magnetic layers ($n * n * n_m$), $n_m = 4$ magnetic planes each ($k = 1 - 4, 8 - 11$), pinhole ($m * m * 5$), $n = 13$, $m = 5$.

$$|S_{i,j,k}| = B_s \left(\frac{|H_{i,j,k}|}{4T} \right), \quad (2)$$

$$B_s(x) = \frac{3}{2} \coth\left(\frac{3x}{2}\right) - \frac{1}{2} \coth\left(\frac{x}{2}\right). \quad (3)$$

At each grid location (i, j, k) the local field according to Eq. (1) has to be calculated. The angle of $\vec{H}_{i,j,k}$ supplies the new direction $\alpha_{i,j,k}$ and the Brillouin function yields the magnitude $|S_{i,j,k}|$ of the spin. The spin is aligned until a local energy minimum is reached. The procedure is repeated until the corresponding magnetization changes ΔM drop below a limit of 10^{-6} . The magnetization itself then is given by

$$M = \frac{1}{8n^2 + 3m^2} \sum_{k=1}^{11} \sum_{i=1}^N \sum_{j=1}^N S_{i,j,k} \cos \alpha_{i,j,k}, \quad (4)$$

$$N = \begin{cases} n & 7 < k < 5 \\ m & 4 < k < 8 \end{cases}$$

Periodic boundary conditions are used in the (i, j) planes of the magnetic layers. No contributions to the local field are considered outside the magnetic body on the planes (1,11) of the magnetic layers and (5,6,7) of the pinhole (see Fig. 1).

The number of iterations can be reduced considerably by introducing successive overrelaxation with ω parameters close to the stability limit of $\omega = 2$.

$$\alpha_{i,j,k}^{\text{new}} := \alpha_{i,j,k}^{\text{old}} + \omega (\alpha_{i,j,k}^{\text{new}} - \alpha_{i,j,k}^{\text{old}})$$

ω	1.0	1.5	1.9	1.97
number of iteration loops	2007	954	224	75

III. SIMPLE MODEL WITHOUT PINHOLES

In this approach the spin direction is fixed within the n_m planes of each magnetic layer. The energy then is given by

$$E = -2n_m H_a \cos \alpha + J_{al} \cos(2\alpha) + J_{aq} \cos^2(2\alpha). \quad (5)$$

The minimum of the energy E is achieved by differentiating the energy equation: $dE/d\alpha = 0$. The magnetization curve $M(H_a)$ results in the parameterized form

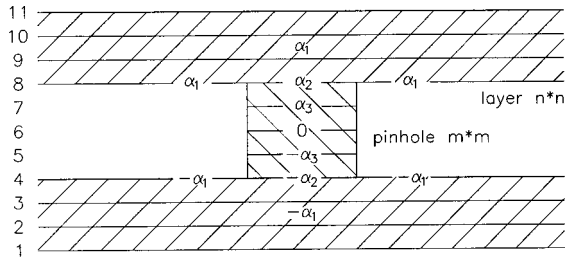


FIG. 2. Sketch for the simplified lattice model.

$$H_a = \frac{2}{n_m} \cos \alpha [J_{al} + 2J_{aq} \cos(2\alpha)], \quad M = \cos \alpha. \quad (6)$$

During evaluation of Eq. (6) the angle in the region $0 \leq \alpha \leq \pi/2$ is preselected first, both the magnetization $M(\alpha)$ and $H_a(\alpha)$ can be calculated according to Eq. (6). M increases linearly with H_a in the case of $J_{aq}=0$, the saturation field H_{a_s} only depends on J_{al} and n_m :

$$M(H_a) = \begin{cases} \frac{n_m}{2J_{al}} H_a & 0 \leq H_a \leq H_{a_s} \\ 1 & H_a \geq H_{a_s} \end{cases}, \quad H_{a_s} = \frac{2J_{al}}{n_m}. \quad (7)$$

IV. SIMPLIFIED LATTICE MODEL

The lattice calculations show, that the angles α_i in some regions are constant for a given external field. Only in the plane above and below the pinhole, the angles start already turning to the other side. That implies a model with constant α_i values in well-defined regions (Fig. 2) and the approximation for the total energy including f and af coupling. This model allows a fast calculation also in the pinhole case. The energy then is given by

$$\begin{aligned} E = & -H_a \cos \alpha_1 (8n^2 - 2m^2) - 2m^2 H_a \cos \alpha_2 \\ & - 2m^2 H_a \cos \alpha_3 - 2m^2 J_f \cos(\alpha_2 - \alpha_3) \\ & - 2m^2 J_f \cos \alpha_3 - 2J_f \cos(\alpha_1 - \alpha_2) \left\{ \frac{m^2}{4m} + (n^2 \right. \\ & \left. - m^2) J_{al} \cos 2\alpha_1 + (n^2 - m^2) J_{aq} \cos^2 2\alpha_1. \right. \end{aligned} \quad (8)$$

In Eq. (6), lines 1–2 contain the Zeeman term, line 3 the f coupling (planes 4–8) and lines 5–6 the af coupling (planes 4,8), line 4 the f coupling within the planes 4,8. In the two cases considered these spins are coupled over the area (m^2) or along the edge ($4m$). In the first case the model agrees better with the lattice model at the bigger pinholes (3×3), in the last at the smaller ones (1×1). (The results are presented in the Figs. 4 and 5.)

The minimum of the energy is achieved by differentiating the energy with respect to the unknown angles α_i :

$$f_i = \frac{\partial E}{\partial \alpha_i} = 0, \quad \mathbf{f}'_{ij} = \frac{\partial f_i}{\partial \alpha_j}. \quad (9)$$

The nonlinear system of equations $f_i=0$ was solved according to an iterative procedure, using the Jacobian-matrix \mathbf{f}' .

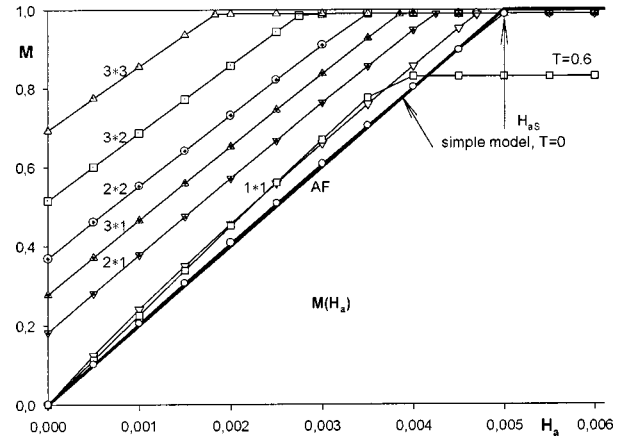


FIG. 3. $M(H)$ -curves, two magnetic layers $16 \times 16 \times 4$, several p pinhole sizes $m_x \times m_y \times 5$, $J_{al} = 10^{-2}$, $J_{aq} = 0$, $T = 0.287$ if not signed otherwise, comparison with the simple model [Eq. (7)].

$$\mathbf{f}' \Delta \vec{\alpha} = -\vec{f} \rightarrow \vec{\alpha}_{j+1} = \vec{\alpha}_j + \Delta \vec{\alpha}. \quad (10)$$

As starting values we used $\alpha_1 = \alpha_2 = 1$, $\alpha_3 = 1/2$. The contributions of the spins in the different areas must be added to get the magnetization M :

$$M = \frac{(8n^2 - 2m^2) \cos \alpha_1 + 2m^2 (\cos \alpha_2 + \cos \alpha_3) + m^2}{8n^2 + 3m^2}. \quad (11)$$

V. RESULTS

In Fig. 3 we show the influence of different pinhole sizes on the $M(H)$ curve for $J_{aq}=0$. Without pinhole, the lattice calculation and the simple model [Eqs. (6) and (7)] agree very well due to the rigid spin configuration. Increasing the size of the pinhole causes the remanence to increase considerably, reaching around 70% of saturation for a pinhole covering less than 4% of the considered area. This is in agreement with the literature,⁴ where similar effects have been reported. Due to a parallel decrease of the saturation field, however, the slope of the $M(H)$ curve remains nearly unchanged. It is interesting to note, that the lattice calculation result in a zero remanence for the smallest pinhole (1×1) considered in Fig. 3. The small ferromagnetic coupling mediated by the pinhole in this case is not strong enough, to cause a ferromagnetic behavior of a part of the film stack. The curve for the temperature $T=0.6$ shows the expected decrease of both the saturation field and magnetization.

This changes as soon as biquadratic coupling is included in the calculations. In Fig. 4 we show magnetization curves for two ratios of J_{al} and J_{aq} and the three models for the smallest pinhole. Although $J_{al} > 2J_{aq}$ in Fig. 3, which leads to zero remanence following the simplest model of Eqs. (6) and (7), even the smallest pinhole now causes a nonzero remanence. This can be understood in terms of a weakening of the bilinear coupling due to the presence of the pinhole. In terms of the correlation between roughness,⁵ loose spins at the interfaces and biquadratic coupling this implies, that imperfect films are more sensible even to extremely small pinholes.

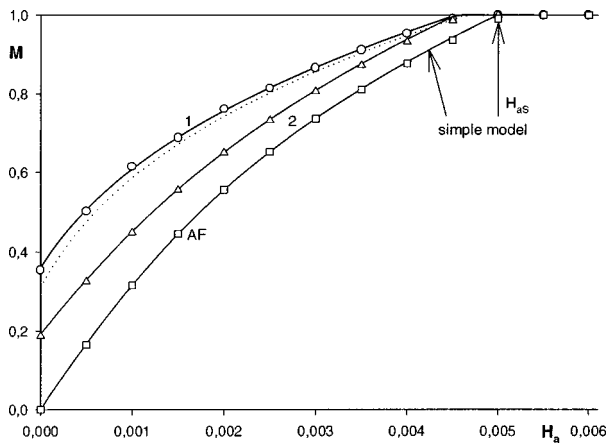


FIG. 4. $M(H)$ curves, $T=0$, planes 16×16 , pinhole 1×1 or af, comparison between lattice calculations (circles, triangles, squares), simple model [solid, Eq. (6)] and the model of Sec. IV, coupling over the area (dotted) and edge (solid), curves 1: $J_{al}=6 \times 10^{-3}$, $J_{aq}=2 \times 10^{-3}$, curves 2: $J_{al}=8 \times 10^{-3}$, $J_{aq}=10^{-3}$.

The comparison of the results of the different models shown in Fig. 4 shows, that the simplified description of Eqs. (8)–(11) reproduce the results of the full lattice calculations very reasonably. Obviously, the optimized grid of Fig. 2 is a good model for the degrees of freedom which have to be taken into account. Note, that the scaling of the simple model for the saturation field [Eq. (6), $J_{al}+2J_{aq}$] still holds in the presence of pinholes (Figs. 4 and 5). The smaller J_{al} allows a larger remanent magnetization (compare curve 1 with curve 2 in Fig. 4, also the solid and dotted curves in Fig. 5). Similar as already reported in the literature,⁴ the coupling over the edges of the pinhole produces results that are closer to the full lattice calculations. This is checked again in Fig. 5, where the influence of the pinhole size is shown. An increase of the edge length of the pinhole by a factor of 1.5 causes the remanence to increase from 0.19 to 0.3. A direct correlation, however, can, up to now, not be established. Further work concerning this point and the temperature dependence of $M(H)$ is in progress.

VI. FINAL CONSIDERATION

We discussed the influence of pinholes on the magnetization curves of coupled multilayers using full lattice calcu-

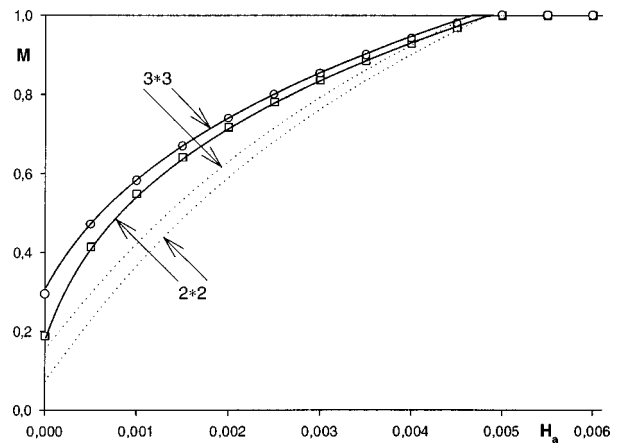


FIG. 5. $M(H)$ curves, comparison between lattice calculations (circles, squares) and the model of Sec. IV, layers $48 \times 48 \times 4$, pinhole $m \times m \times 5$, coupling over the area, $J_{al}=6 \times 10^{-3}$, $J_{aq}=2 \times 10^{-3}$ (solid); $J_{al}=8 \times 10^{-3}$, $J_{aq}=10^{-3}$ (dotted).

lations known from the literature and an optimized model which enables extremely fast calculations. Both bilinear as well as biquadratic coupling have been included. The results show, that the presence of the biquadratic coupling can enhance the influence of the pinhole which implies a larger sensitivity of imperfect films to magnetic shorts between the layers. Additionally, we demonstrated that the optimized model reproduces the results of the full lattice calculations with very high accuracy. There are three advantages of the simplified lattice model: (1) the faster calculations now offer the opportunity to include complex structures with much more grid points, (2) more physical insight about the relevant coupling paths (e.g., edge or area), (3) improvement of the full lattice model through better initial values. This algorithm — controlled by the full lattice model — could enable a very fast and reliable modeling of coupled films with defects.

¹J.-F. Bobo, M. Piecuch, and E. Snoeck, *J. Magn. Magn. Mater.* **126**, 440 (1993).
²D. B. Fulghum and R. E. Camley, *Phys. Rev. B* **52**, 13436 (1995).
³H. Kikuchi, J.-F. Bobo, and R. L. White, *IEEE Trans. Magn.* **33**, 3583 (1997).
⁴C. H. Marrows, R. Loloee, and B. J. Hickey, *J. Magn. Magn. Mater.* **184**, 137 (1998).
⁵J. C. Slonczewski, *J. Magn. Magn. Mater.* **150**, 13 (1995).